EAJM 2013; 45: 50-7 The Eurasian Journal of Medicine **Review**

Abdominal Perfusion Computed Tomography

Abdominal Perfüzyon Bilgisayarlı Tomografi

Hayri Ogul[1], Ummugulsum Bayraktutan[1], Yesim Kizrak[1], Berhan Pirimoglu[1], Zeynep Yuceler[1], M. Erdem Sagsoz[3], Omer Yilmaz[2], Bulent Aydinli[2], Gurkan Ozturk[2], Mecit Kantarci[1]

[1]Department of Radiology, School of Medicine, Atatürk University, Erzurum, Turkey
[2]Department of General Surgery, School of Medicine, Atatürk University, Erzurum, Turkey
[3]Department of Biophysics, School of Medicine, Atatürk University, Erzurum, Turkey

Abstract

The purpose of this article is to provide an up to date review on the spectrum of applications of perfusion computed tomography (CT) in the abdomen. New imaging techniques have been developed with the objective of obtaining a structural and functional analysis of different organs. Recently, perfusion CT has aroused the interest of many researchers who are studying the applicability of imaging modalities in the evaluation of abdominal organs and diseases. Perfusion CT enables fast, non-invasive imaging of the tumor vascular physiology. Moreover, it can act as an *in vivo* biomarker of tumor-related angiogenesis.

Key Words: Abdominal perfusion, Computed tomography

Özet

Bu çalışmanın amacı batında perfüzyon bilgisayarlı tomografi (BT) uygulama spektrumuna çağdaş bir yaklaşım sağlamaktır. Yeni görüntüleme teknikleri sadece organların yapısını değerlendirmek için değil aynı zamanda farklı organların fonksiyonel analizlerini yapmak için de geliştirildi. Son zamanlarda, geliştirilen bu cihazlar arasında perfüzyon BT abdominal organların ve hastalıkların değerlendirilmesinde bu gibi görüntüleme modalitelerinin uygulanabilirliğinde çoğu araştırmacının ilgisini çekti. Perfüzyon BT tümörün vasküler fizyolojisini tanımlama olanağı sağlar. O non-invazivdir ve onun uygulaması ve analizi kolaydır. Dahası, O tümör ilişkili anjiogenezin *in-vivo* biyolojik belirleyicisi olarak davranabilir.

Anahtar Kelimeler: Abdominal perfüzyon, Bilgisayarlı tomografi

Introduction

The field of radiology has had recent developments such as the advent of multidetector computed tomography (MDCT), among other imaging methods, that have allowed for consequential acquisition of images with higher quality and accuracy. Perfusion CT is an exciting CT technology that permits the functional evaluation of tissue vascularity. It has been generally used since the development of imaging techniques and post-processing software. Perfusion CT measures the temporal changes in the tissue density after intravenous injection of a contrast medium bolus using a series of dynamically acquired CT images [1]. In this article, the authors review the basic principles and technique of perfusion CT and discuss its various oncologic and nononcologic clinical applications in abdominal imaging.

Dual-energy CT

Dual-energy CT enables differentiation of the materials and tissues in the images obtained based on the differences in the iodine and water densities; the resulting CT images are reconstructed using two different energy spectra. Dual energy CT can be performed with multidetector CT imaging in current clinical settings. An advantage of dual-energy CT is its ability to perform scanning at low tube voltages (kVp). There are four types (GE Healthcare, Siemens, Philips and Toshiba) of dual-energy CT systems. Dual-energy CT imaging is used routinely in clinical abdominal imaging. The Siemens dual-energy CT system has two X-ray sources and two X-ray detectors that are offset by 90° with a single CT gantry. This system has the advantage of better energy separation compared with the fast kV switching system.

Dual-energy CT offers more specific tissue characterization in the obtained CT images and can improve the assessment of vascular disease. Dual-energy material decomposition images offer improved visualization of vascular structures and abnormal calcifications, such as renal and gall stones, as well as depiction of soft tissue structures, such as the kidneys, pancreas, liver, and spleen. These images have the potential to increase the sensitivity and specificity of pathology detection [2].

Received: May 7, 2012 / **Accepted:** June 16, 2012

Correspondence to: Mecit Kantarci, 200 Evler Mah. 14. Sok. No: 5 Dadaskent, Erzurum, Turkey
Phone: +90 442 231 69 15 Fax: +90 442 236 13 01 e-mail: akkanrad@hotmail.com
doi:10.5152/eajm.2013.09

Perfusion CT

CT perfusion imaging is a developing technique for quantitatively evaluating tissue blood perfusion [1]. Perfusion CT is a minimally invasive method that has the advantage of providing highly reliable quantification of parenchymal perfusion at a low cost. Perfusion CT is performed by the acquisition of serial images after bolus injection of an iodinated contrast agent. The mean transit time (MTT) and permeability surface area product (PS) of the contrast material are two important parameters for perfusion CT. These parameters describe parenchymal microvascular changes. MTT is defined as the time that a contrast agent takes to go through the liver, from entry to exit, averaged over all possible paths. The PS is defined as the speed of transfer of a contrast agent from the capillary endothelium to the intercellular space [3]. The time to peak (TTP), measured in seconds, is defined as the time elapsed before peak enhancement is achieved.

Hepatic perfusion CT enables the analysis of liver function and the measurement of the following: tissue blood flow (Tissue BF; mL/min/100 g); tissue blood volume (Tissue BV; mL/100 g); and MTT (s). This method is designed to calculate hepatic blood flow and portal blood flow using a color-encoded display of parameters from the liver time-density curve using an iodine contrast agent. Thus, liver functional maps are calculated from the input function based on regions of interest (ROIs) over the aorta and portal vein [2].

Perfusion Imaging of the Liver

Vascular anatomy of the normal liver

It is important to understand the complex blood flow through the liver. The liver has a dual afferent blood supply; it receives an afferent blood supply through both the portal vein and hepatic artery. Tributaries of the portal vein include the splenic and inferior and superior mesenteric veins. The PV delivers ~ 75% of the afferent blood volume to the liver. Within the liver, the portal vein splits into right and left branches. The terminal circulation is observed in microscopic slides as portal veins in the portal tracts. The other source of blood coming into the liver originates from the common hepatic artery, which is one of the three branches of the celiac trunk. The hepatic artery delivers highly oxygenated blood to the liver and accounts for 20-25% of the total afferent blood volume. Sinusoids are the largest microvascular circulation components of the liver. The sinusoids of the liver drain directly into the terminal hepatic venules. The terminal hepatic venules eventually coalesce to form large hepatic veins. The right, left, and middle hepatic veins form the venous drainage, and these three vessels form a confluence that drains into the inferior vena cava.

Perfusion imaging in cirrhosis

Hepatic cirrhosis is diffuse liver disease characterized by progressive destruction and distortion of the normal lobular architecture of the liver parenchyma. The hemodynamic end result of cirrhosis is progressive obstruction of the intrahepatic vascular bed by fibrosis and nodular regeneration, resulting in portal hypertension [4]. This increase in the intrahepatic vascular resistance leads to a decrease in the portal fraction of liver perfusion. This decreased portal perfusion is partially compensated by an increase in the arterial flow, while the total liver perfusion is reduced in cirrhotic patients [3, 5].

CT can reliably demonstrate the varied hemodynamic concomitants of portal hypertension, including a panorama of portosystemic venous collaterals, splenomegaly and ascites. Because of their high spatial and temporal resolution, modern CT scanners have been widely used to measure perfusion in clinical studies, diagnosis and treatment assessment. To evaluate the quantitative and qualitative microvascular alterations in liver cirrhosis, hepatic perfusion parameters (both MTT and PS) are measured in patients with liver cirrhosis by perfusion CT. These parameters are important and critical for assessing the function of the liver, as shown by many studies in humans and animals. The MTT mainly reflects the transit time through the capillaries. In the some studies [3, 6], the MTT values observed in control subjects were higher than those observed in cirrhotic patients. However, other studies [7, 8] reported no difference in the MTT of controls versus cirrhotic patients. Van Beers et al. [9] reported that the total liver perfusion (TLP) is decreased in patients with cirrhosis and non-cirrhotic chronic liver disease, while the hepatic arterial perfusion index (HPI) and MTT are increased.

Perfusion imaging for detection of hepatocellular carcinoma

Hepatocellular carcinoma (HCC) is the most common malignant neoplasm of the liver in many parts of the world. This neoplasm is often a hypervascular tumor that derives its blood supply primarily from the hepatic artery. CT angiography is a sensitive method for the detection of intranodular arterial and portal perfusion flow and, thus, enables the accurate diagnosis of HCC [10]. The typical vascular pattern of HCC is high attenuation relative to the liver parenchyma during the early phase of dynamic CT [11]. Using perfusion CT to measure tumor perfusion and assess HCC is beneficial for determining the differential diagnosis, evaluating tumor aggressiveness, monitoring the therapeutic effects, and determining the final patient outcome [1,3]. The perfusion parameters of HCC differ considerably from the background liver parenchyma. HCC has higher BF, BV and PS values and lower MTT values than the background liver [12] (Figure 1).

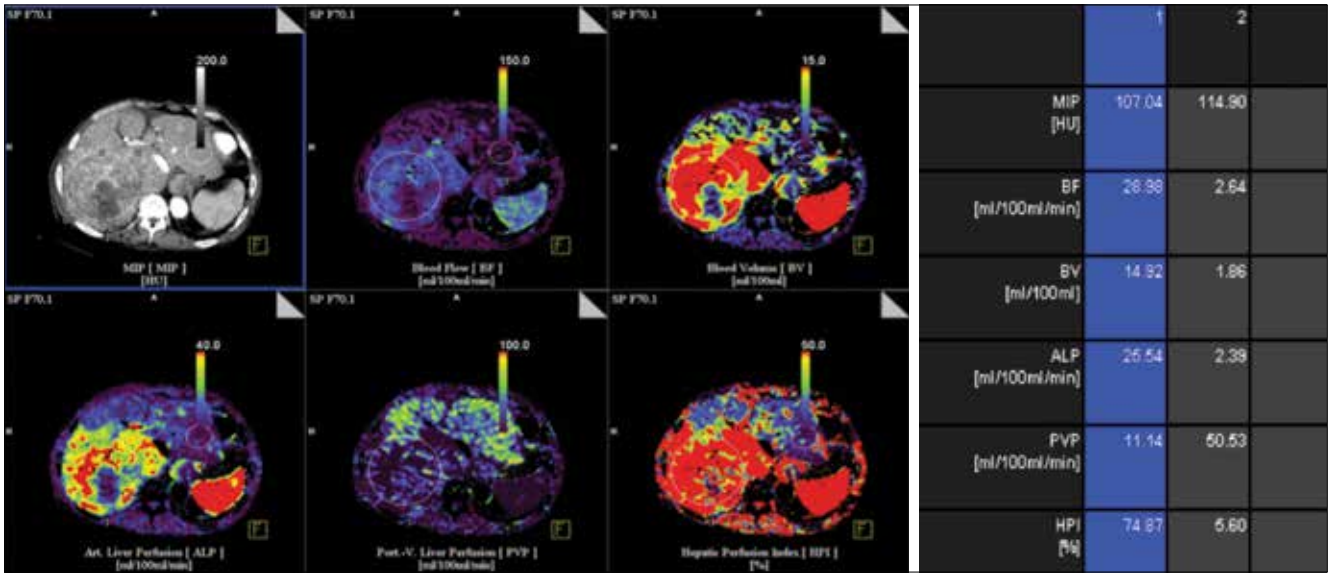

Figure 1. *Transverse contrast material functional CT perfusion color map of BF of CT perfusion in a patient with HCC in right lobe of liver. Various ROIs in tumor (1) and normal liver (2) were drawn Transverse CT perfusion functional maps of BF, BV, ALP, PVP, and HPI in 65-year-old man show large mass in right lobe of liver that has a distinct range of colors compared with background liver parenchyma.*

Perfusion imaging for metastatic disease

Identification of hepatic metastatic disease is very important for its staging, prognosis and treatment. Perfusion CT can reveal increased arterial perfusion in patients with hepatic metastatic disease [13, 14]. Routine CT imaging is insensitive to occult and early stage hepatic micro metastases. Perfusion CT is more sensitive in the characterization of focal hepatic lesions and in the early detection of liver metastases that are too small to be detected by conventional CT [14]. Increases in both the HAP and HPI reveal the possibility of liver micro metastasis [15]. The presence of higher perfusion in the metastatic lesions, identified by CT imaging, is considered a good prognostic indicator, suggesting that the patient will have an optimal response to treatment [1, 14] (Figure 2).

Perfusion imaging in liver transplantation

Living-donor liver transplantation has been developed as a treatment for patients with end-stage liver diseases. Living-donor liver transplantation using right lobe grafts is widely accepted as the standard procedure. This transplantation procedure may lead to hemodynamic alterations, especially hepatic venous congestion. Hepatic venous congestion usually takes place in the anterior segment as a result of ligation of the large middle hepatic vein tributaries, including the veins of segment V or VIII.

Multiphase contrast enhanced CT, Doppler ultrasonography, and MRI are all used to non-invasively evaluate hepatic venous congestion after liver transplantation [16-18]. However, these imaging modalities can hardly provide quantitative measurements of segmental congestion. CT perfusion imaging is a quantitative method for identifying liver hemodynamic properties [19, 20]. It can monitor the pattern of hemodynamic changes in the portal vein and hepatic artery, contributing to the early diagnosis of blood vessel complications after transplantation [15]. Qian et al. [20] reported that CT liver perfusion imaging enables the feasible quantification of the hemodynamic alterations in right-lobe liver grafts after living-donor liver transplantation. Researchers have suggested that ligation of large MHV tributaries, compared to small middle hepatic vein tributaries, can bring about a more marked perfusion imbalance between the anterior and posterior segments.

Perfusion Imaging of the Pancreas

Ultrasonography, computed tomography, and magnetic resonance imaging have been used to evaluate and characterize pancreatic pathologies [21]. Due to technical advances in the development of multidetector and multiphase contrast-enhanced computed tomography, CT imaging is becoming the first-line imaging procedure of choice for pancreatic disease diagnostics [22].

Perfusion CT protocol for the pancreas

Usually, patients receive water (500 mL) perorally before examination to distend the stomach and duodenum, creating a better delineation of the pancreas. Afterwards, a craniocaudal topogram scan is performed (100 kVp, 35 mAs, and 0.6 mm slice thickness), followed by a non-contrast-enhanced scan (100 kVp, 100 mAs, 5 mm slice thickness, 0.9 pitch, and 0.5 s

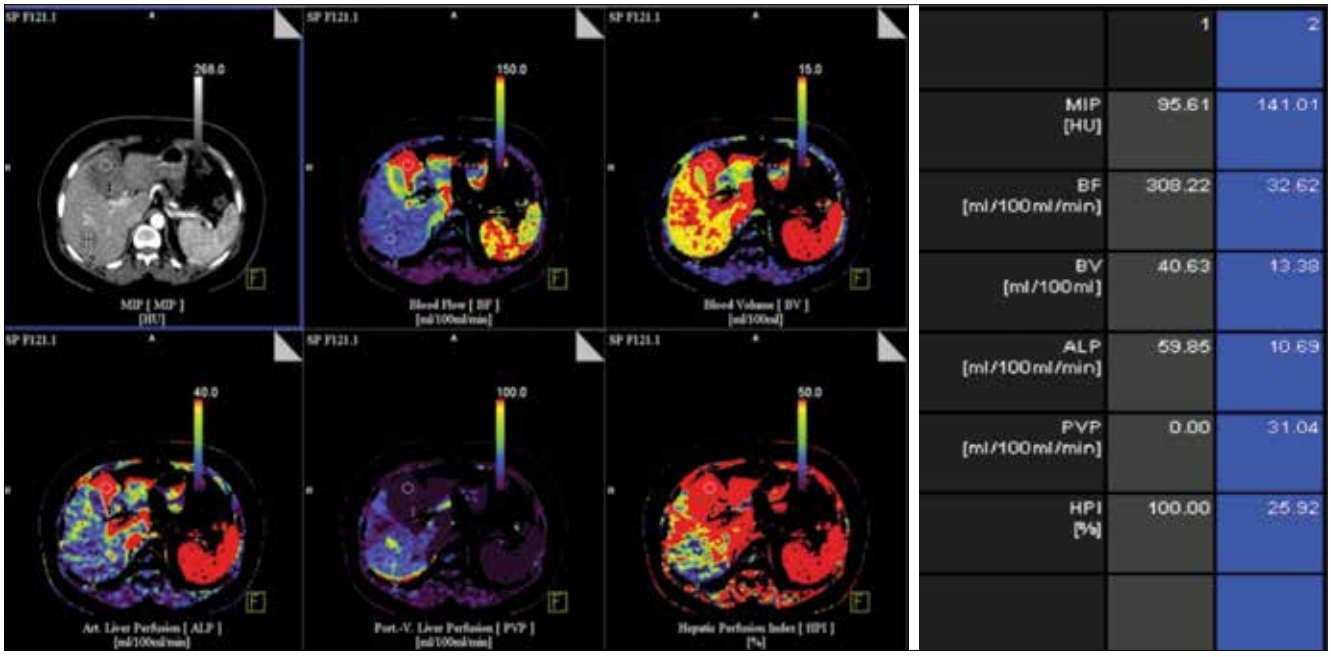

Figure 2. *Transverse contrast-enhanced CT image and functional CT perfusion map of BF, BV, ALP, PVP, and HPI in 45 year-old woman with liver metastasis from pankreas Ca show high BF, BV, ALP compared with normal liver parenchyma.*

rotation time). A dynamic study of the selected area (including the whole pancreas) is performed in a single breath-hold at the end of expiration after contrast injection (100 kVp, 145 mAs, 5 mm slice thickness, 376 mm field-of-view, 148 mm z-axis range, and 0.28 s rotation time). Iodinated contrast material (50 mL iodixanol, 320 mg iodine/mL) is administered through an 18-gauge intravenous cannula using a dual-head pump injector at a flow rate of 5 mL/s, followed by a flush with sterile saline solution (50 mL, 5 mL/s) [22-24].

Perfusion CT in evaluating pathologies of the pancreas

The most common pathologies of the pancreas include inflammatory processes (such as acute and chronic pancreatitis) and neoplastic diseases (of which pancreatic adenocarcinoma is the most common). The identification of these lesions has significant therapeutic and prognostic implications [23]. Without tissue sampling, the differential diagnosis of pancreatic pathologies by conventional CT remains a challenge. One of the most recent developments in CT imaging is body and organ perfusion CT. Perfusion CT provides information about the tissue hemodynamics and can assess parameters such as the tissue blood perfusion and permeability, leading to a better, non-invasive characterization and identification of (tumor) tissues. Perfusion CT imaging has previously been investigated, but it was only investigated in pancreatic adenocarcinoma [24, 25]. Poor vascularization is characteristic of pancreatic adenocarcinoma [26, 27]. Pancreatic adenocarcinoma usually presents as a hypodense region relative to the surrounding normal parenchyma by conventional CT imaging or can instead be isoattenuating (up to 11% of pancreatic adenocarcinoma) [28, 29].

There are no or very few functional microvessels remaining in necrotic and cystic tissue areas, resulting in low perfusion values [30] (Figure 3). Indeed, the perfusion values in necrotic adenocarcinoma tissue, pseudocystic tissue, and acute pancreatitis zones are significantly lower than the values obtained in the surrounding tissue [25]. Additionally, neuroendocrine tumor tissue has a significantly higher blood flow and blood volume than normal pancreatic tissue. Neuroendocrine tumors are hyperdense by conventional CT because they are higher vascularized [31]. d'Assignies et al. [24] measured CT perfusion parameters in pancreatic endocrine tumors and found higher blood flow values (239.8 mL/100 g/min, 23.9 mL/100 g, and 54.9 mL/100 g/min for the blood flow, blood volume, and permeability surface area product, respectively).

Differential diagnosis between pancreatitis and pancreatic adenocarcinoma based solely on perfusion CT parameter values remains troublesome. However, clinical symptoms and patient history also have to be taken into account [31]. Distinguishing acute and chronic pancreatitis based on perfusion CT parameters remains troublesome; significantly decreased perfusion values were obtained only in active, acute pancreatitis focal lesions. However, the combination of CT and clinical information (e.g., the prototypical sudden

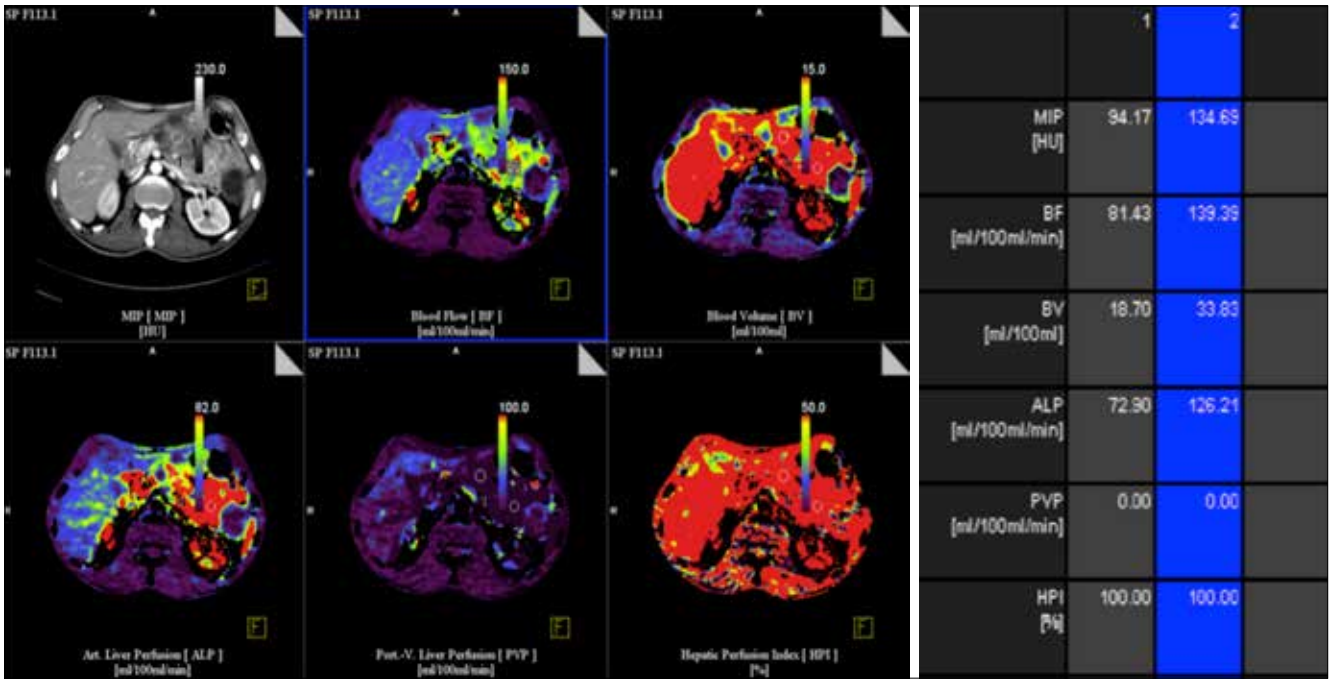

Figure 3. *Transverse contrast-enhanced CT image and functional CT perfusion map in 60 year-old woman with serous cyctic adenoma show low BF, BV, ALP compared with normal liver parenchyma. Various ROIs in tumor (1) and normal pancreas (2) were drawn.*

onset of acute pancreatitis) can help in sorting through the differential diagnosis to identify these diseases [32].

Perfusion Imaging of the Kidney

Renal perfusion is an essential functional parameter for evaluating renal vascular damage in patients with renal artery stenosis, ureteral obstruction, chronic allograft rejection, and other renal diseases [33, 34]. Kidney hypoperfusion can potentially trigger mechanisms leading to renal injuries and, ultimately, altered renal function [35, 36]. Several imaging modalities have been proposed for the noninvasive assessment of renal perfusion, including dynamic contrast-enhanced MRI, contrast-enhanced US, and contrast-enhanced CT [37]. Multidetector CT is a useful tool for measuring renal perfusion. Multidetector CT is largely available, and the relationship between the measured renal tissue attenuation and the concentration of the contrast medium is strictly linear [24, 38]. To date, the measurement of renal perfusion has predominately been validated with an extended gamma variate model, providing regional RBF and glomerular filtration rate measurements. This model requires a high rate of contrast medium injection (e.g., 15 mL/sec) to produce a bolus injection time that is as short as possible [39]. This high-rate injection is impossible to deliver with a peripheral catheter because of the small diameter of the peripheral vein; therefore, a central venous catheter is mandatory, which is invasive and cannot be used easily in routine clinical practice. Thus, a validation of the renal perfusion measurement after low-rate contrast medium injection is mandatory for applying multidetector CT in clinical practice [40]. CT renal perfusion imaging is feasible and delivers a reliable qualitative and quantitative analysis of the normal renal cortex and renal pathological perfusion.

Perfusion CT protocol of the kidney

First, an unenhanced CT scan of the upper abdomen at the level of the kidneys, as determined by the topogram, is performed. For perfusion imaging, iopromide (50 mL) is injected through an 18-gauge needle into an antecubital vein at a flow rate of 5 mL/s followed by 20 mL of saline solution at the same flow rate. Scanning is usually initiated after a 6-second delay to allow for acquisition of baseline nonenhanced images [40].

Perfusion CT in pathologies of the kidney

The contrast material administered with the CT scan is infused i.v. and perfuses the venous system before passing to the arterial system. When the contrast material reaches the kidneys, it passes through the major renal arteries to the interlobar, arcuate, and then interlobular arteries. The contrast material then passes through the afferent arterioles, the glomerular tuft and, finally, to the efferent arterioles. From

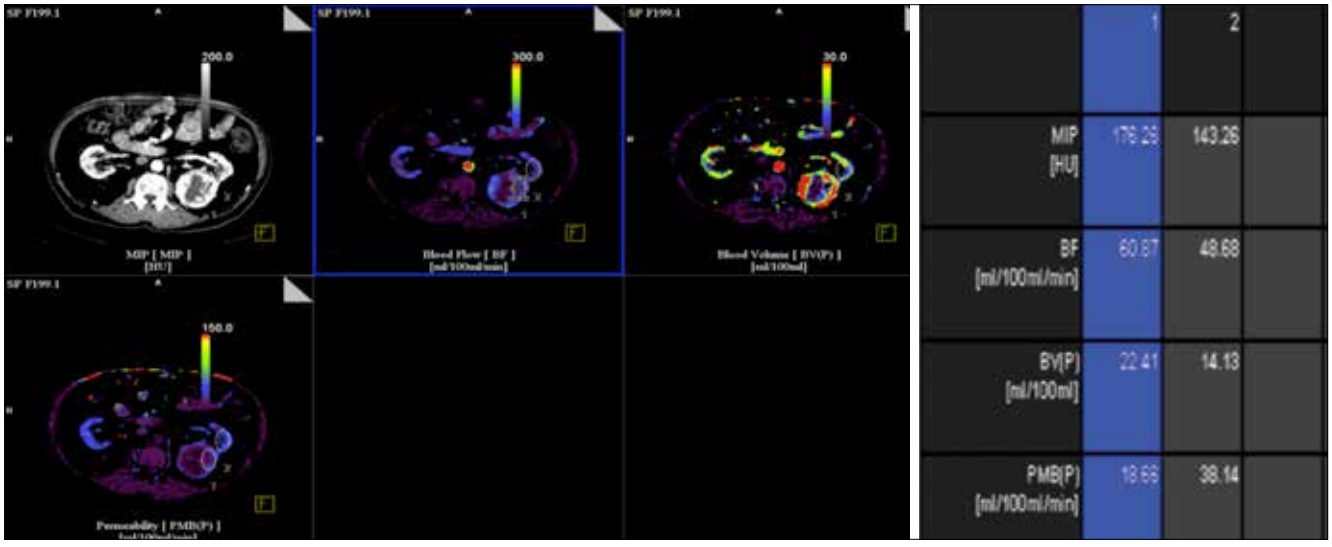

Figure 4. *Transverse contrast-enhanced CT image and functional CT perfusion map in 80 year-old man with RCC.Two regions of interest, selected on RCC(ROI 1), normal ipsilateral renal cortex (ROI 2). Blood colour maps (Blood Volume, BV; Blood Flow, BF; Permeability) show mass in left kidney that has a distinct range of colors compared with renal cortex.*

the juxtamedullary glomeruli, the contrast material passes through the efferent arterioles to the descending vasa recta and then to the outer and inner medulla to form the tubular capillary bed [41]. Theoretically, if we could measure the concentration of the contrast material over time during its vascular passage through the kidney, starting from the major vessels to the renal pelvis, the perfusion and function of each part of the kidney could be identified and measured separately [40, 41]. By measuring the contrast opacification, or the radio density in different parts of the kidney, the contrast concentration can be estimated [42]. Chen et al. [43] reported CT perfusion values for normal renal cortex; they found average values of 454.32 mL x min^{-1}x 100 g^{-1} for the BF and 23.53 mL x 100 g^{-1} for the BV, and the mean values of the BF and BV were significantly higher while the MTT was significantly lower in renal cell carcinoma (RCC) than in normal renal cortex.

Renal cell carcinoma is the most common malignant tumor of the kidney; most cases of RCC are hypervascular. Angiogenesis plays an important role in the growth and spread of RCC [44]. As an appropriate noninvasive tool for the assessment of angiogenesis, perfusion CT is becoming widely used for the diagnosis of cancers and for the monitoring of the tumor response to therapy [44, 45]. Kaneoya analyzed the functional CT images of 14 RCCs and found a significant linear correlation with the functional CT parameters (BF, BV and MTT) [46]. Patients with metastatic RCC have a poor prognosis with a 5-year survival rate of less than 10% [47]. Ng et al. [48] reported that there was a significant increase in the tumor blood flow and a significant reduction in the tumor MTT in metastatic RCC (Figure 4).

Conclusion

MDCT has a high temporal and spatial resolution in the measurement of perfusion. Additionally, MDCT enables the simultaneous measurement of perfusion in multiple organs. Perfusion CT is becoming a preferred functional imaging tool in the field of oncology, and it has the potential to play a crucial role in the management of cancer patients, particularly as a means of monitoring their response to antiangiogenic drugs. Moreover, the indications for perfusion CT include differentiating between inflammatory processes and tumor-like lesions, determining the degree of function in certain organs, and detecting the presence of residual tumor tissue after minimally invasive therapies.

Conflict of interest statement: The authors declare that they have no conflict of interest to the publication of this article.

References

1. Kambadakone AR, Sahani DV. Body perfusion CT: technique, clinical applications, and advances. Radiol Clin North Am 2009; 47: 161-78. **[CrossRef]**
2. Okada M, Kim T, Murakami T. Hepatocellular nodules in liver cirrhosis: state of the art CT evaluation (perfusion CT/volume helical shuttle scan/dual-energy CT, etc.). Abdom Imaging 2011; 36: 273-81. **[CrossRef]**
3. Chen ML, Zeng QY, Huo JW, et al. Assessment of the hepatic microvascular changes in liver cirrhosis by perfusion computed tomography. World J Gastroenterol 2009; 15: 3532-7.
4. Waller III RM, ThoOliver TW, McCain AH, et al. Computed tomography and sonography of hepatic cirrhosis and portal hypertension. Radiographics 1984; 4; 677-715.

5. Kleber G, Steudel N, Behrmann C, et al. Hepatic arterial flow volume and reserve in patients with cirrhosis: use of intra-arterial Doppler and adenosine infusion. Gastroenterology 1999; 116: 906-14. [CrossRef]
6. He W, He Q. Hepatic perfusion parameters in cirrhosis: dynamic CT measurements correlated with portal vein CT angiography [A]. In: the Radiological Society of North America: RSNA 2003 Scientific Papers 2003: Q08-Q1267.
7. Guan S, Zhao WD, Zhou KR, et al. CT perfusion at early stage of hepatic diffuse disease. World J Gastroenterol 2005; 11: 3465-7.
8. Hashimoto K, Murakami T, Dono K, et al. Assessment of the severity of liver disease and fibrotic change: the usefulness of hepatic CT perfusion imaging. Oncol Rep 2006; 16: 677-83.
9. Van Beers BE, Leconte I, Materne R, Smith AM, Jamart J, Horsmans Y. Hepatic perfusion parameters in chronic liver disease: dynamic CT measurements correlated with disease severity. AJR Am J Roentgenol 2001; 176: 667-73.
10. Merine D, Takayasu K, Wakao F. Detection of hepatocellular carcinoma: comparison of CT during arterial portography with CT after intraarterial injection of iodized oil. Radiology 1990; 175:707-10.
11. Hayashi M, Matsui O, Ueda K, et al. Correlation between the blood supply and grade of malignancy of hepatocellular nodules associated with liver cirrhosis: evaluation by CT during intraarterial injection of contrast medium.AJR Am J Roentgenol 1999; 172: 969-76.
12. Sahani DV, Holalkere NS, Mueller PR, et al. Advanced hepatocellular carcinoma: CT perfusion of liver and tumor tissue—initial experience. Radiology 2007;243:736-43. [CrossRef]
13. Blomley MJ, Coulden R, Dawson P, et al. Liver perfusion tudied with ultrafast CT. J Comput Assist Tomogr 1995; 19: 424-33. [CrossRef]
14. Miles KA, Hayball MP, Dixon AK. Functional images of hepatic perfusion obtained with dynamic CT. Radiology 1993; 188: 405-11.
15. Zhong L, Wang WJ, Xu JR. Clinical application of hepatic CT perfusion. World J Gastroenterol 2009; 15: 907-11. [CrossRef]
16. Kim KW, Kim TK, Kim SY, et al. Doppler sonographic abnormalities suggestive of venous congestion in the right lobe graft of living donor liver transplant recipients. AJR Am J Roentgenol 2007; 188: 239-45. [CrossRef]
17. Yamamoto H, Maetani Y, Kiuchi T, et al. Background and clinical impact of tissue congestion in right-lobe living-donor liver grafts: a magnetic resonance imaging study. Transplantation 2003; 76: 164-9. [CrossRef]
18. Park EA, Lee JM, Kim SH, et al. Hepatic venous congestion after right-lobe living-donor liver transplantation: the added value of delayed-phase imaging on CT. J Comput Assist Tomogr 2007; 31: 181-7. [CrossRef]
19. Pandharipande PV, Krinsky GA, Rusinek H, Lee VS. Perfusion imaging of the liver: current challenges and future goals. Radiology 2005; 234: 661-73. [CrossRef]
20. Qian LJ, Zhuang ZG, Cheng YF, Xia Q, Zhang JJ, Xu JR. Hemodynamic alterations in anterior segment of liver graft after right-lobe living-donor liver transplantation: computed tomography perfusion imaging findings. Abdom Imaging 2010; 35: 522-7. [CrossRef]
21. Zamboni GA, D'Onofrio M, Principe F, Pozzi Mucelli R. Focal pancreatic lesions: accuracy and complications of US-guided fineneedle aspiration cytology. Abdom Imaging 2010; 35: 362-6. [CrossRef]
22. Miura F, Takada T, Amano H, Yoshida M, Furui S, Takeshita K. Diagnosis of pancreatic cancer. HPB (Oxford) 2006; 8: 337-42. [CrossRef]
23. Bellizzi AM, Frankel WL. Pancreatic pathology: a practical review. Labmedicine 2009; 40: 417-26.
24. d'Assignies G, Couvelard A, Bahrami S, et al. Pancreatic endocrine tumors: tumor blood flow assessed with perfusion CT reflects angiogenesis and correlates with prognostic factors. Radiology 2009; 250: 407-16. [CrossRef]
25. Delrue L, Blanckaert P, Mertens D, Cesmeli E, Ceelen WP, Duyck P. Assessment of tumor vascularization in pancreatic adenocarcinoma using 128-slice perfusion CT imaging. J Comput Assist Tomogr 2011; 35: 434-8. [CrossRef]
26. Erkan MM, Reiser-Erkan C, Michalski CW, et al. Cancerstellate cell interactions perpetuate the hypoxia-fibrosis cycle in pancreatic ductal adenocarcinoma. Neoplasia 2009; 11: 497-508.
27. Masamune A, Shimosegawa T. Signal transduction in pancreatic stellate cells. J Gastroenterol 2009; 44: 249-60. [CrossRef]
28. Prokesch RW, Schima W, Chow LC, Jeffrey RB. Multidetector CT of pancreatic adenocarcinoma: diagnostic advances and therapeutic relevance. Eur Radiol 2003; 13: 2147-54. [CrossRef]
29. Prokesch RW, Chow LC, Beaulieu CF, Bammer R, Jeffrey RB Jr. Isoattenuating pancreatic adenocarcinoma at multi-detector row CT: secondary signs. Radiology 2002; 224: 764-8. [CrossRef]
30. Lasson A, Jönsson K, Lore'n I, Sternby NH. The proteolytic effect of pancreatic pseudocyst fluid on vessel walls. Int J Pancreatol 1994; 16: 23-9.
31. Ricke J, Hänninen EL, Amthauer H, Lemke A, Felix R. Assessment of the vascularization of neuroendocrine tumors by stimulated acoustic emission of SHU 508A ultrasound contrast agent and color or power Doppler sonography. Invest Radiol 2000; 35: 253-9. [CrossRef]
32. Swaroop VS, Chari ST, Clain JE. Severe acute pancreatitis. JAMA 2004; 291: 2865-8. [CrossRef]
33. Lee VS, Rusinek H, Bokacheva L, et al. Renal function measurements from MR renography and a simplifi ed multicompartmental model. Am J Physiol Renal Physiol 2007; 292: 1548-59. [CrossRef]
34. Pereira RS, Gonul II, McLaughlin K, et al. Assessment of chronic renal allograft nephropathy using contrast-enhanced MRI: a pilot study. AJR Am J Roentgenol 2010; 194: 407-13. [CrossRef]
35. Pelaez LI, Juncos LA, Stulak JM, Lerman LO, Romero JC. Noninvasive evaluation of bilateral renal regional blood fl ow and tubular dynamics during acute unilateral ureteral obstruction. Nephrol Dial Transplant 2005; 20: 83-8 . [CrossRef]
36. Grenier N, Quaia E, Prasad PV, Juillard L. Radiology imaging of renal structure and function by computed tomography, magnetic resonance imaging, and ultrasound. Semin Nucl Med 2011; 41: 45-60. [CrossRef]
37. Miles KA. Perfusion CT for the assessment of tumour vascularity: which protocol? Br J Radiol 2003; 76: 36-42. [CrossRef]
38. Yi CA, Lee KS, Kim EA, et al. Solitary pulmonary nodules: dynamic enhanced multi-detector row CT study and comparison with vascular endothelial growth factor and microvessel density. Radiology 2004; 233: 191-9. [CrossRef]
39. Krier JD, Ritman EL, Bajzer Z, et al. Noninvasive measurement of concurrent single-kidney perfusion, glomerular fi ltration, and tubular function. Am J Physiol Renal Physiol 2001;281:630-8.
40. Lemoine S, Papillard M, Belloi A, et al. Renal perfusion: noninvasive measurement with multidetector CT versus fluorescent microspheres in a pig model. Radiology 2011; 260: 414-20. [CrossRef]

41. Helck A, Sommer WH, Klotz E, et al. Determination of glomerular filtration rate using dynamic CT-angiography: simultaneous acquisition of morphological and functional information. Invest Radiol 2010; 45: 387-92.
42. Goh V, Halligan S, Bartram CI. Quantitative tumor perfusion assessment with multidetector CT: are measurements from two commercial software packages interchangeable? Radiology 2007; 242: 777-82. **[CrossRef]**
43. Chen Y, Zhang J, Dai J, Feng X, Lu H, Zhou C. Angiogenesis of renal cell carcinoma: perfusion CT findings. Abdom Imaging 2010; 35: 622-8. **[CrossRef]**
44. Goh V, Dattani M, Farwell J, et al. Radiation dose from volumetric helical perfusion CT of the thorax, abdomen or pelvis. Eur Radiol 2011; 21: 974-81. **[CrossRef]**
45. Wildberger JE, Adam G, Boeckmann W, et al. Computed tomography characterization of renal cell tumors in correlation with histopathology. Invest Radiol 1997; 32: 596-601. **[CrossRef]**
46. Kaneoya K, Ueda T, Suito H, et al. Functional computed tomography imaging of tumor-induced angiogenesis: preliminary results of new tracer kinetic modeling using a computer discretization approach. Radiat Med 2008; 26: 213-22. **[CrossRef]**
47. Yildiz E, Ayan S, Goze F, Gokce G, Gultekin EY. Relation of microvessel density with microvascular invasion, metastasis and prognosis in renal cell carcinoma. BJU Int 2008; 101: 758-64. **[CrossRef]**
48. Ng CS, Wang X, Faria SC, Lin E, Charnsangavej C, Tannir NM. Perfusion CT in Patients With Metastatic Renal Cell Carcinoma Treated With Interferon. AJR 2010; 194: 166-71. **[CrossRef]**